Send Orders of Reprints at reprints@benthamscience.net

Current Physical Chemistry, **2013,** *3,* **187-198**

Interaction and Reaction of the Antioxidant Mn^{III} [*Meso*-Tetrakis(4-*N*-MethyI Pyridinium) Porphyrin] with the Apoptosis Reporter Lipid Phosphatidylserine

Juliana C. Araújo-Chaves[1,2], Cintia Kawai[1], Antonio F. A. A. Melo[5], Katia C. U. Mugnol[1], Otaciro R. Nascimento[3], Jeverson T. Arantes[4], Frank N. Crespilho[5] and Iseli L. Nantes[1,*]

[1]*Centro de Ciências Naturais e Humanas (CCNH), Universidade Federal do ABC, Rua Santa Adélia, 166, Santo André, SP 09210-170, Brazil;* [2]*Centro Interdisciplinar de Investigação Bioquímica (CIIB), Universidade de Mogi das Cruzes, Av. Dr Cândido Xavier de Almeida Souza, 200, Mogi das Cruzes, SP, 08780-911, Brazil;* [3]*Grupo de Biofísica "Sergio Mascarenhas", Universidade de São Paulo, Avenida Trabalhador São-carlense, 400, Sao Carlos, SP, 13560-970, Brazil;* [4]*Centro de Engenharia, Modelagem e Ciências Sociais Aplicadas (CECS) Universidade Federal do ABC, Rua Santa Adélia, 166, Santo André, SP 09210-170, Brazil;* [5]*Instituto de Química de São Carlos, Universidade de São Paulo, Avenida Trabalhador São-carlense, 400, São Carlos, SP, 13560-970, Brazil*

Abstract: In the present study, the binding of the cationic Mn^{III}TMPyP [meso-tetrakis (4-N-methyl pyridinium) porphyrin] to negatively charged membrane models containing phosphatidylcholine (PC)/ phosphatidylserine (PS) and the porphyrin reactivity with PS-derived peroxides (LOOH) were evaluated. This investigation is relevant due to the participation of PS in cell signaling and apoptosis. Addition of PC/PS liposomes to Mn^{III}TMPyP solutions led to spectral changes of the porphyrin electronic absorption spectrum suggestive of electrostatic interactions with the negatively charged interface provided by PS. The binding of Mn^{III}TMPyP to PC/PS liposomes was corroborated by the quenching of the fluorophore merocyanine 540. In addition total energy calculations of saturated and unsaturated PS based on the spin-polarized variant of KS-DFT were used to support some experimental data. Cyclic voltammetry analysis revealed that the association to PC/PS liposomes shifted the redox potential of the Mn^{II}/Mn^{III} (+87 mV *vs* NHE, in aqueous buffered solution) couple to a more positive value to (+110 mV *vs* NHE). This event favors the oxidation of $O_2^{\bullet}$ to O_2 by the porphyrin. Mn^{III}TMPyP was able to react with the lipid-derived peroxides as evidenced by spectral changes of the porphyrin consistent with the generation of a high valence state (Mn^{IV}=O) of the catalyst. The spectral changes were not observed when biological lipids containing unsaturated PC and PS were replaced by the corresponding dipalmitoyl (DP)-derived: DPPC/DPPS.

Keywords: Mn^{III}TMPyP [*meso*-tetrakis (4-*N*-methyl pyridinium) porphyrin], Phosphatidylserine, Liposomes, Electronic absorption spectroscopy fluorescence spectroscopy, Electrostatic interaction, Superoxide dismutase mimetics.

Dedicated to Henrik Bohr on the occasion of his 60th birthday (and published as part of the Quantum Nanobiology and Biophysical Chemistry special issue of CPC).

INTRODUCTION

Phosphatidylserine (PS) is an aminophospholipid that is restricted to the inner leaflet of the plasma membrane of most healthy cells [1-3]. In cell membranes, PS asymmetry results from translocation mechanisms provided by 'flippases' that drive unidirectionally the aminophospholipid to the cytoplasmatic face of the membrane [4-6]. The input of specific lipids by these transporters against concentration gradient requires coupling to ATP hydrolysis. Loss of PS asymmetry, *i.e.*, transbilayer movement of the lipid from the cytoplasmic to the external face of the citoplasmic membranes, is an early manifestation of apoptosis and it is a result of both decreased aminophospholipid translocase activity and activation of a calcium-dependent scramblase, that promotes bidirectional transport of membrane lipids [3-5,7,8]. Scramblases promote a bidirectional transport of lipids driven by a pre-existing transbilayer lipid gradient, and in the plasma membrane these transporters are activated by Ca^{2+}. More details about catalyzed transbilayer lipid movements can be found in the minireview [8]. PS exposure is important for recognition and removal of cellular fragments in the events of erythrocyte senescence, apoptosis and platelet activation [9-11]. PS is probably not the sole ligand identified by phagocytes to remove apoptotic cells and PS exposure also occurs in non apoptotic cells [12-14]. Changes of the PS distribution in the lipid membraine play a role in signal transduction and modulate the activities of several membrane proteins. The PS distribution is also related to Ca^{2+} and Na^{+} uptake; $P2X_7$-stimulated shedding of the homing receptor CD62L, a process required for lymphocyte migration to inflammatory sites [15]; and reversal of activity of the multidrug transporter P-glycoprotein. T lymphocytes that express low levels of the transmembrane tyrosine phosphatase have PS exposed at high levels on the membrane surface. Loss of membrane asymmetry with exposure of PS at cell surface also acts as a

*Address correspondence to this author at the Centro de Ciências Naturais e Humanas (CCNH), Universidade Federal do ABC, Rua Santa Adélia, 166, Santo André, SP 09210-170, Brazil; Tel: +55-11-4996-0174;
E-mail: ilnantes@ufabc.edu.br

1877-9476/13 $58.00+.00

cofactor for the coagulation cascade [16], and has anti-inflammatory or immunosuppressive effects, including the capacity to inhibit macrophage parasiticidal activity and cytokine production, as well as lymphocyte proliferation and cytokine production [17]. On the other hand, exposure of PS on the surface of apoptotic cells has been related to the events of inflammation and coagulation present in patients with systemic lupus erythematosus [18]. Also, non-apoptotic transient exposure of PS has been seem in a diversity of cellular events such as phagocytosis [8], signal transduction of lymphocytes, sperm capacitation [12], myotube formation [19], neutrophil stimulation [20], and in the activation of an ATP-dependent cation channel of immune and some epithelial cells that are known as $P2X_7$ [21,22]. Besides the participation of endogenous PS in cell signaling, it has been demonstrated that PS-containing liposomes are able to inhibit transcription of inducible nitric oxide synthase and nitric oxide production in mouse macrophages [23,24].

Superoxide dismutase (SOD) is part of the antioxidant enzymatic apparatus against oxidative stress in aerobic organisms. Mitochondrial SOD exhibits manganese ion as the catalytic center that promotes the dismutation of superoxide ion according to the following mechanism (Eq. 1 and 2):

$$\text{Enzyme-}Mn^{2+} + O_2^{-\bullet} \rightarrow \text{Enzyme-}Mn^{3+} + H_2O_2 \quad (1)$$

$$\text{Enzyme-}Mn^{3+} + O_2^{-\bullet} \rightarrow \text{Enzyme-}Mn^{2+} + O_2 \quad (2)$$

Due to the intrinsic structure-related barriers such as hypersensitivity reactions, short half-life after subcutaneous or intramuscular injection (99% clearance in <1 hour) and very deficient cellular uptake that impair the use of natural SOD as an antioxidant therapeutic agent [24-31], synthetic SOD mimetics have been the subject of intensive research. The most of SOD mimetics share the structure of metal chelates [32].

Manganese-containing organometallics (two representative structures in Fig. **1**), including manganese-porphyrins, have been characterized as efficient SOD mimetics, despite the predominance of ion superoxide reductase activity – the manganese reduction occurs at expenses of cellular reducing agents such as NADPH and glutathione – and low specificity because they commonly have also peroxidase activity.

Among the therapeutic compounds mimicking SOD, metalloporphyrins have been extensively studied regarding their catalytic mechanisms and capacity for membrane binding with consequences for the biological effects [33,34]. Particularly, manganese porphyrin studies have contributed to the comprehension and understanding of the mechanisms of the antioxidant enzymes, superoxide dismutase [35] and catalase [36-38]. These studies are particularly important because the micro-environmental conditions of cells can shift more or less favorably the desirable antioxidant properties of porphyrins. Due to the close relation of the mitochondria with cell life and death events, several studies have been concerned with the interaction of metallo *meso*-tetrakis cationic porphyrins with mitochondria and membrane models of the organelle [39-41]. Recently, the glutathione peroxidase (GPx), superoxide dismutase (SOD) and cytochrome *c*-like antioxidant activities of *para* Mn^{III}TMPyP in isolated rat liver mitochondria (RLM) and mitoplasts have been reported [42]. The *para* Mn^{III}TMPyP redox potential (+60 mV *vs* NHE) suggests that this porphyrin is less efficient as a SOD mimic relative to the *ortho* isomer (+ 260 mV *vs* NHE) [43-45]. However, in antimicyn A-poisoned mitoplasts representing a model for the generation of the superoxide ion, Mn^{III}TMPyP bound to the inner mitochondrial membrane, efficiently decreased the generation of the prooxidant species [42]. The depletion of glutathione (GSH) with the superoxide ion quenching is consistent with the use of GSH as a reducing agent for high valence states of Mn^{III}TMPyP and so, with glutathione peroxidase (GPx) activity. The porphyrin can also exhibit SOD and cytochrome *c* antioxidant activities. In solution, Mn^{II}TMPyP generated by the xantine/xantine-oxidase system was able to reduce ferric cytochrome *c*. This result suggests a potential to remove the superoxide ion by returning electrons back to the respiratory chain (cytochrome *c*-like activity). Most of Mn^{II}TMPyP is expected to be produced at the expense of NADPH/GSH depletion and so, electron transfer from Mn^{II}TMPyP to respiratory cytochromes occurs at the expense of cell reducing agents. Therefore, the principal antioxidant contribution of Mn^{III}TMPyP is the GPx-like activity the efficiency of which is dependent on the NADPH/GSH content in the cells [42].

The action of Mn^{III}TMPyP on the cell redox balance is intrinsically related to the redox potential of the Mn^{II}/Mn^{III} couple that, in turn, can be modulated by association with the membrane lipid bilayers [41,46]. Despite the affinity of TMPyP for the cardiolipin (CL)-rich inner mitochondrial membrane, access to the organelle is obligatorily preceded by passage through the plasmatic membrane and in the cytosol the cationic porphyrin might potentially bind PS, asymmetrically segregated to the inner leaflet. Previously, a

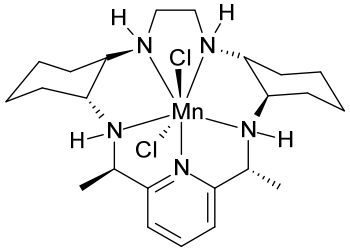

M40403

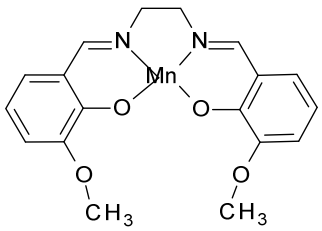

Mn(III)salen EUK-113

Fig. (1). Structures of two non-porphyrinic SOD mimetics.

putative oxidative action of cytochrome *c* on PS contributing to the phospholipid externalization had been proposed and so, a similar effect could be promoted by a cationic metalloporphyrin [47]. Therefore, considering the relevant biological roles played by PS in the clearance of apoptosis, cell signaling, and signal transduction [48] and the impact of manganese porphyrins in the redox-sensitive signaling molecules [34], the binding and reactivity of Mn^{III}TMPyP with this phospholipid in different PS-containing membrane models were investigated.

MATERIALS AND METHODS

Chemicals

Mesotetrakis porphyrin (Chart 1) was purchased from Mid Century Chemicals (Posen, IL, USA). PC (natural egg and synthetic dipalmitoil form) and PS (natural porcine brain and synthetic dipalmitoil form) were purchased from Avanti Polar Lipids (Alabaster, AL, USA) and HEPES was purchased from Sigma-Aldrich Corp. (St. Louis, MO, USA).

Liposome extruder and extrusion membranes were also purchased from Avanti Polar Lipids and liposomes were prepared with membranes of 400 nm pore.

Electronic Absorption Spectra Measurements

The electronic absorption spectra of porphyrins were measured during reaction with peroxides by using a Shimadzu Model 1501 MultiSpec (Tokyo, Japan) employing the photodiode array scan mode. The spectral resolution was 0.5 nm, and the spectra were obtained at time intervals of 1 second. The optical path length was 1 cm for all measurements. The temporal conversion of Mn^{III}TMPyP was measured by absorbance decay at 400 nm. The exponential decay curves obtained were best fit to eq. 1 using Origin 8.1 software (OriginLab Corporation, MA, USA), where eq. 1 is given by

$$y = y_{\infty} + \mathrm{A}e^{-x.\mathrm{k}_{obs}}, \quad (1)$$

where y and y_{∞} are the absorbance at 400 nm at a given time and at infinite time, respectively, and k_{obs} is the observed first-order rate of porphyrin conversion to high valence state.

Determination of the Dissociation Constants

Binding constants for the interaction of Mn^{III}TMPyP with liposomes were determined using the fluorescence quenching data (emission percentage as a function of porphyrin concentration) of merocyanine 540 (MC540). The quenching data were analyzed based on eq. 2,, which is given by

$$Y = Y_{max}\frac{x^n}{\mathrm{K}^n + x^n}, \quad (2)$$

where Y is the quenching percentage at one porphyrin concentration, Y_{max} is the maximal quenching percentage that corresponds to the fraction of occupied binding sites, K is the dissociation constant, x is the porphyrin concentration, and n is the cooperative coefficient.

The data were also adjusted by a semi-log plot and by the Hill equation, eq. 3, which is given by

$$\log\left(\frac{Y}{1-Y}\right) = n\log x - \log \mathrm{K}, \quad (3)$$

where Y is the % of saturated binding sites, x represents the porphyrin concentration, and n is the Hill coefficient that indicates in actual binding titrations the degree of cooperativity.

Equation 2 was also used to fit the spectral changes of the porphyrin promoted by the titration with lipids (PC/PS liposomes).

Cyclic Voltammetry

Measurements were taken using a potentiostat/ galvanostat μAutolab with the GPES software and a three electrode experimental setup. The working electrode was a glassy carbon electrode (3 mm diameter, Bioanalytical Systems), a platinum sheet was the auxiliary electrode, and $Ag/AgCl_{sat}$ was the reference electrode. Prior to each measurement, the working electrode was cleaned with 0.3 $\mu mol.L^{-1}$ alumina, rinsed with a stream of distilled water, wiped with tissue paper, and immersed in 2.5 mL of the solution containing 0.05 $mol.L^{-1}$ phosphate buffer (pH 7.4), 0.1 $mol.L^{-1}$ NaCl, and 0.5 $mmol.L^{-1}$ Mn porphyrin. The scan rates are indicated in the figures, and the voltammograms were obtained by scanning the potential from the most negative to the most positive values and back, typically in the region of - 600 to 1200 mV *vs* Ag/AgCl.

Theoretical Calculations

The theoretical results were obtained *via* total energy KSDFT calculations based on the spin-polarized variant of KS-DFT, within the LDA, and employing the projected augmented wave method (PAW) [49]. A plane wave basis set expansion up to 464.51 eV, as implemented in the VASP code, was used [50]. All atoms were allowed to relax until the forces in each Cartesian coordinate became smaller than 0.025 eV/A°. Similar conditions was user in the study of the phorphirin interaction with ditetradecyldimethylammonium bromide (DTDAB) [51]. A unit cell with dimensions of 30, 30 e 40 Å in x, y, and z directions, respectively, was used to prevent spurious interactions between its images in our periodic boundary condition calculations.

RESULTS AND DISCUSSION

Binding of TMPyP to PS-containing Membrane Model

Fig. (**2**) shows that Mn^{III}TMPyP interacts with the negatively charged interface provided by PC/PS (80 and 20% weight, respectively) liposomes [52]. The electronic absorption (EA) spectra of Mn^{III}TMPyP in both homogeneous and heterogeneous (PC/PS liposomes) media result from the contribution of CT and π-π* electronic transitions. The presence of manganese ion as the metal center changes the energy of the π-*d* transition and consequently decreases the large overlap of the LMCT (ligand to metal charge transfer) and Soret bands typically present in the EA spectrum of the iron ion partner porphyrin [53,54]. The interaction with negatively charged PC/PS liposomes slightly changes the energy of both π-*d* and π-π*

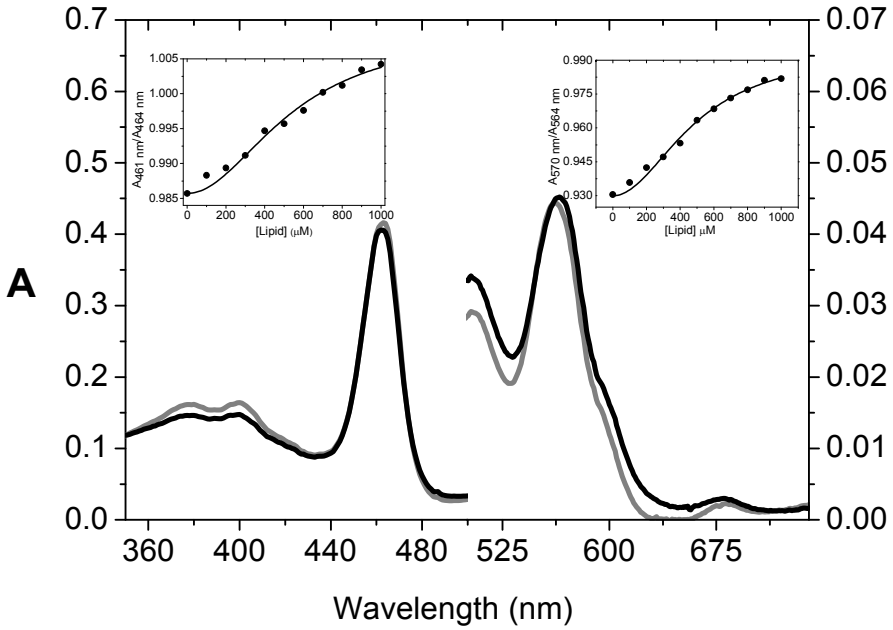

Fig. (2). Spectral changes of Mn^{III}TMPyP in the absence (gray line) and in the presence (black line) of 1 mmol.L^{-1} total lipid in PC/PS liposomes. The insets shows 461/464 nm absorbance ratios in the CT band (left) and the 570/564 nm absorbance ratios in the Q band (right) obtained by the titration of the porphyrin with crescent amounts of PC/PS liposomes.

transitions leading to discrete shifts of the CT and Q bands that could be better evaluated by analyzing the respective 461/464 nm and 570/564 nm intensity ratios. The association with liposomes also slightly decreased the molar absorptivity of the Soret band (π-π* transitions contribution) of the porphyrin. These spectral changes are expected from an electrostatic interaction of the positively charged Mn^{III}TMPyP meso-ligands with the negatively charged interface of PC/PS rather than from a porphyrin moiety buried in the bilayer. Changes in the Q and CT intensity ratios were obtained from a titration of the porphyrin with PC/PS liposomes and ploted as a function of lipid concentration (insets of Fig. **2**). The insets of Fig. (**2**) show the effect of lipid concentration on the Q and CT intensity ratios. For both bands, a sigmoid profile suggestive of cooperativity was obtained. The data were well fitted by using eq. 1 (Materials and Methods) with n = 2 and K around 500 nmol.L^{-1}.

The interaction of Mn^{III}TMPyP with PS-containing liposomes was probed by using the fluorescent probe MC540. MC540 is an amphiphilic fluorescent (Fig. **3**) probe that is sensitive to the environment and lipid packing [55]. MC540 emits a strong 585 nm fluorescence when partitioned in fluid phase phospholipids. The fluorescence peak at 585 nm is also dominant in lipid phosphatidylcholine (PC) monolayers when the fluorophore is compressed to a surface density of less than 70 A^2 per POPC lipid molecule and less than 60 A^2 per DPPC lipid molecule. MC-540 dissolved in water or in a gel-phase vesicle suspension exhibits a broad emission peak centering at 572 nm. Fluorescence emission peaking at 572 nm is also observed for MC540 in POPC and DPPC monolayers adjusted to an area per molecule greater than 70 A^2. The charged group in MC540 is restricted to the functional sulfonate group and the charge delocalization through lipid-dye interactions is responsible for the sensitivity of the dye to the packing state of the lipids [55]. In the present study, the binding was assessed by the degree of fluorescence quenching as a function of porphyrin concentration, and the effect on the bilayer organization was evaluated by the changes in the MC540 fluorescence spectrum promoted by the porphyrin. Fig. (**4A**) shows the effect of Mn^{III}TMPyP concentration on the fluorescence quenching of MC540 in PC/PS liposomes. A *plateau* of fluorescence quenching was observed at Mn^{III}TMPyP concentrations higher than 2 μmol.L^{-1}. Also the binding isotherm obtained by plotting the fraction of saturated binding sites (Y) as a function of the log of Mn^{III}TMPyP gave a sigmoid profile consistent with a positive cooperativity (Fig. **4B**). The binding isotherms were treated using the Hill-type cooperative model (eq. 2), which allows the determination of the dissociation constant (K) and of the n coefficient (Inset of Fig. **4B**). Both binding isotherm fitting and the Hill plot resulted in K ~ 1 μM and n ~ 2. The positive cooperativity might result from an expected capacity

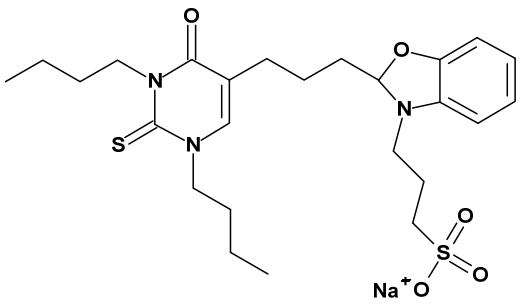

Fig. (3). Structure of MC540.

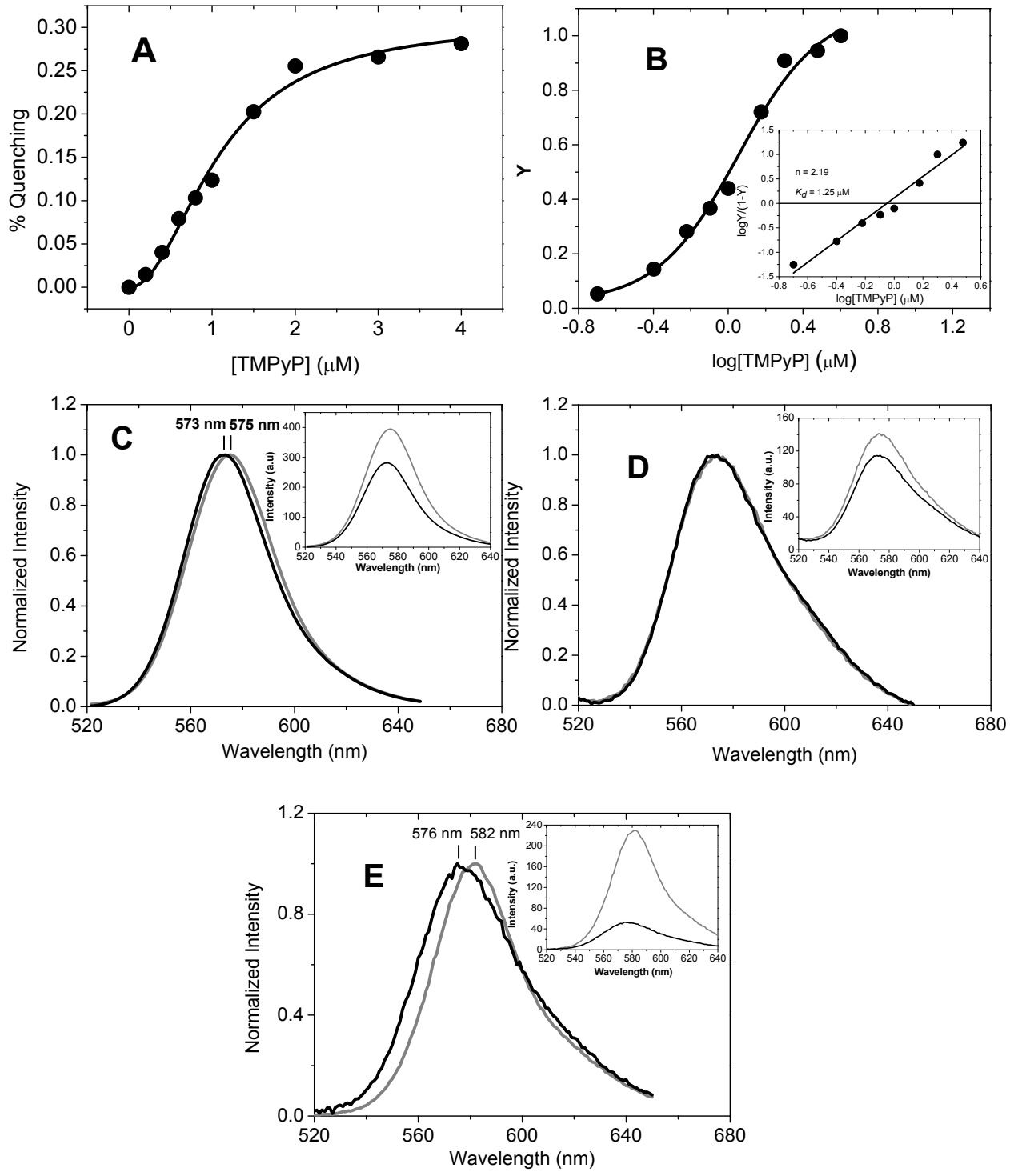

Fig. (4). Effect of Mn^{III}TMPyP on the binding and the percentage of saturation of the manganese porphyrin in PC/PS liposomes. **A** - Quenching of relative fluorescence intensity (RFI) of MC540 promoted by the interaction of Mn^{III}TMPyP with PC/PS liposomes. **B** – Percentage of fractional superficial saturation as function of porphyrin concentration. The inset shows the Hill plot obtained for the binding of Mn^{III}TMPyP to PC/PS liposomes. Binding isotherms show cooperative profiles and were fitted using a cooperative-binding model. **C**- Normalized spectra of MC50 before (gray line) and after (black line) the addition of Mn^{III}TMPyP at the concentration of saturation. - **D** and **E** show the MC540 normalized spectra obtained in the presence of 100% PS and DPPC/DPPS (saturated lipids) vesicles, respectively. The insets show the original spectra in which it is possible to see the quenching of MC540 fluorescence by the porphyrin. The experiments were carried out using 1mM PC/PS liposomes containing 80% 20% weight of PC and PS, respectively, in 5 $mmol.L^{-1}$ phosphate buffer at pH 7.0. The experiments were carried out using 10 $\mu mol.L^{-1}$ MC540.

of Mn^{III}TMPyP to promote demixing of negatively-charged PS and constituting domains that favor the association of additional porphyrin molecules. Also, the association of the cationic porphyrin with the negatively charged moieties of the PS head group could decrease the apparent pK_a of the PS amino group because the neutralization of the negative charges. In this condition, the increase of deprotonated amino groups could also contribute for the binding of additional porphyrin molecules. It is important to consider that the electrostatic interactions are attenuated by the aqueous environment and strongly interacting hydrogen bonded network of water molecules can contribute for the association of molecular structures [56]. The effect of Mn^{III}TMPyP binding to PC/PS on the MC540 fluorescence spectrum is consistent with the dye partition in membrane with different packing [57,58]. Also, the binding of Mn^{III}TMPyP to PS-containing vesicles was investigated by using saturated lipids (DPPC/DPPS) at the same lipid types ratio used for biological unsaturated lipids (80/20 % weight). In addition, the binding of Mn^{III}TMPyP to 100% PS vesicles was also investigated (Figs. **4C** and **4D**). Fig. (**4C**) shows the spectrum of MC540 in PC/PS vesicles before and after the addition of 4 μmol.L^{-1} Mn^{III}TMPyP. The analyses of the normalized overlapped spectra (gray and black lines, respectively) revealed partial (28%) quenching of the dye emission promoted by the porphyrin binding. In this condition, the reminiscent spectrum presented a 2 nm blue shift of the fluorescence maximum (from 575 to 573 nm). This result is consistent with a preferential partition of MC40 in the bulk water and thus with the fluorescence unaffected by the porphyrin preferentially bound to the membrane. Interestingly, in 100% PS vesicles, the maximal quenching of MC promoted by Mn^{III}TMPyP was 20% and not accompanied by a shift of the fluorescence band (Fig. **4D**). Considering the high negative potential that is expected for the surface of a 100% PS liposome [59], a very low partition of MC in this type of liposome was expected. The spectral changes of MC540 fluorescence were also analyzed for DPPC/DPPS vesicles (Fig. **4E**). The addition of Mn^{III}TMPyP resulted in a 6 nm blue shift of the fluorescence peak (from 582 to 576 nm) associated with a 70% quenching of the emission intensity. This result is consistent with a high partition of MC540 in DPPC/DPPS liposomes where the dye is close enough to the porphyrin for the occurrence of excitation energy transfer. DPPC and DPPS have 41°C and 54°C as the melting point, respectively. For the corresponding natural lipids, with a high content of polyunsaturated fatty acids composition, it is expected a melting point below zero. The highest partition of MC450 in DPPC/DPPS vesicles making possible the highest quenching by the bound porphyrin is according to previous studies of Hao Yu and Sek-Wen Hui, 1992 [55]. In that paper the authors report the higher partition of MC40 in DPPC (36%) than in DOPC (16%) monolayers at pressure 9 dyne/cm, slightly above to that necessary to promote the liquid expanded/liquid condensed (LE/LC) transition in DPPC. The intensity of MC540 quenching by Mn^{III}TMPyP proportional to the percentage of the dye partition in the different lipid bilayer compositions is according to a high affinity of the porphyrin for all the vesicle types investigated here. However, it was considered the possibility of subtle differences in the interaction of saturated and unsaturated PS with Mn^{III}TMPyP. Therefore, total energy KS-DFT calculations based on the spin-polarized variant of KS-DFT, within the LDA, and employing the projected augmented wave method (PAW) were run for saturated and unsaturated PS [49]. The isolated saturated PS molecule (gas phase) converged with curved and divergent acyl chains. One acyl chain converged with a more curved feature than other. The optimized configuration obtained for saturated PS structure is represented in Fig. (**5A**) as a ball and stick. The inter-chains carbon-carbon distances in the asymmetrically curved acyl chains of PS are shown in Fig. (**5B**). The greatest carbon-carbon distance was found for the methyl terminal pair. Following in the direction from the methyl terminal carbon-carbon pair to the head group, the carbon-carbon distances decreased non-linearly up to the half of the acyl chain length wherein the distances were found to vary randomly. Although in the real lipid bilayer the inter-acyl chains carbon-carbon distances of PS can be shorter, it is probable that the asymmetrically curved structure is preserved. This theoretical result is consistent with the MC540 fluorescence spectrum peaking at 582 nm obtained in DPPC/DPPS liposomes (Fig. **4E**). A DPPS structure with divergent and asymmetrically curved acyl chains is expected to create domains of lower lipid packing that allows high partition of the dye in the bilayers where it is strongly quenched by the membrane-associated porphyrin. Theoretical calculations were also run for unsaturated PS. Fig. (**5C**) shows the comparison of Ω3 calculated for saturated (black line) and unsaturated (red line) PS. Significant difference of Ω3 was observed only in the unsaturated carbons. Slight difference was also observed in the head group. This result, consistently with experimental data, suggests that the presence of unsaturated acyl chain is not expected to produce significant effects on the affinity of Mn^{III}TMPyP by the PS-containing membranes but can influence the partition of MC540 on the bilayers since the probe is expected to be intercalated in the membrane.

Fig. (**6**) shows the cyclic voltammograms of Mn^{III}TMPyP in the absence (A) and in the presence of PC/PS liposomes (B and C) obtained by using glass carbon in 5 mmol.L^{-1} phosphate buffer pH 7.4 at 100 mV/s rate in the absence and in the presence of PC/PS liposomes. The voltammograms were obtained by using $Ag/AgCl_{sat}$ as reference electrode and the redox potentials were converted to values *vs* NHE (+ 197 units added) for comparison with literature data. As the PC/PS liposomes does not exhibit redox processes (data not shown) all processes were assigned to the porphyrin (Fig. **6A**). Similarly to the data presented in literature [43, 60] one reversible redox process was detected with $E_{1/2}$ = +87 mV *vs* NHE. It corresponds to a simple one electron process:

$$Mn^{II}TMPyP(H_2O)_2^{4+} \leftrightarrows Mn^{III}TMPyP(H_2O)_2^{5+} + e^-$$

Additionally, it was detected one quasi-reversible one-electron redox process with $E_{pa}2$ = +927 and $E_{pc}1$= +647 mV *vs* NHE, which could correspond to the metal-centered one electron redox process:

$$Mn^{III}TMPyP(H_2O)_2^{5+} \leftrightarrows O{=}Mn^{IV}TMPyP(H_2O)^{4+} + e^- + 2H^+$$

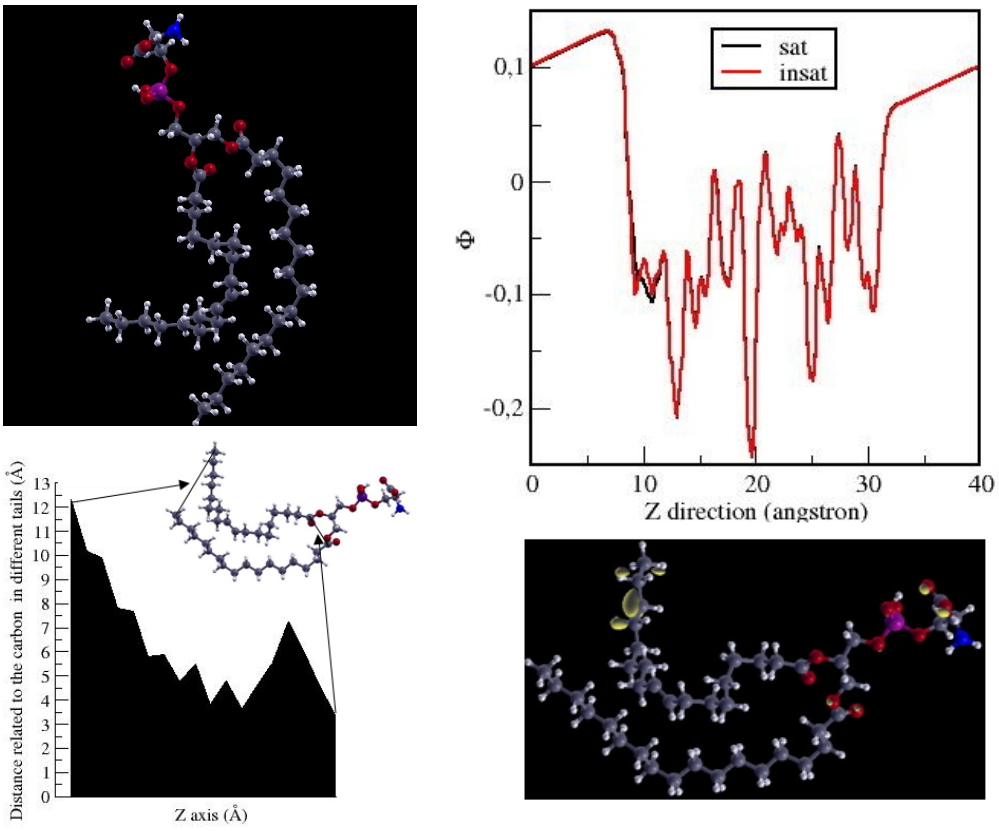

Fig. (5). A - Ball an stick model of saturated PS. The white spheres represent the hydrogen atoms, gray = carbon atoms, red = oxygen atoms, blue = nitrogen atoms and violet = phosphor atom; **B** - Inter-chain carbon-carbon distances for DPPS. **C** - Charge distribution for saturated and unsaturated PS. (Upper panel) The integrated electrostatic potential in X,Y plane versus Z direction . (Lower panel) Charge difference from the saturated and unsaturated molecule. The isosurface value used was 0.2 (electrons/Å^3).

This process has been found in literature as a reversible process. However, in our experimental condition, *i.e.*, in air equilibrated solution, the process was found as a quasi-reversible process. Also, anodic peak ($E_{pa}3$) at +1280 mV *vs* NHE and catodic peak ($E_{pc}3$) at -230 mV *vs* NHE were detected and they might be associated to ring-centered redox processes.

The association of Mn^{III}TMPyP to PC/PS liposomes (Fig, **6B**) led to the disappearance of the putative ring-centered redox process ($E_{pa}3$ and $E_{pc}3$) that could be derived from aggregated states of the porphyrin. Interestingly, the metal-centered reversible process was 20 mV shifted to a more positive value and the $E_{1/2}$ of Mn^{II}/Mn^{III} redox couple was found to be 117 mV vs NHE. Also, $E_{pa}2$ and $E_{pc}1$ were 50 mV shifted to more positive values and they were found as being +977 mV and +697 mV vs NHE, respectively. The acidic microenvironment provided by the negatively charged PC/PS liposomes head groups contributes to the positive redox potential shifts of the manganese-centered redox process of *para* Mn^{III}TMPyP. A similar effect is expected for the association of the porphyrin with the CL-containing inner mitochondrial membrane and consistent with the previously published study in which we observed an efficient effect against superoxide ion generated in antimicyn A-poisoned mitoplasts [42].

Previously, Ferrer-Sueta *et al.* [44] reported that the increase of pH from 7.8 to 11, decreased 94 mV the $E_{1/2}$ of Mn^{II}/Mn^{III} redox process of *ortho* Mn^{III}TMPyP (from 220 mV *vs* NHE to 126 mV *vs* NHE) with a minor effect (-10 mV $E_{1/2}$ shift) for the *meta* and *para* isomers (from 42 and 50 mV *vs* NHE to 52 and 60 mV *vs* NHE, respectively), the latter, the object of the present study. This differentiated effect was assigned to the lower pK_a of manganese-coordinated water of the *ortho* Mn^{III}TMPyP that, in this condition, makes this isomer mainly monohydroxo at pH 11.0 in contrast with the *para* isomer that remained mainly as the aqua form. At pH 11, only an 8 mV difference was observed in the $E_{1/2}$ of Mn^{III}/Mn^{IV} redox process and therefore, the amazing *ortho* effect was significantly diminished for this redox couple. Interestingly, in the present study, a mimic of the *ortho* effect was achieved for *para* Mn^{III}TMPyP by the association with PC/PS liposomes at physiological pH (+110 mV *vs* NHE). Furthermore, the *ortho* effect was here also observed for the Mn^{III}/Mn^{IV} (probably Mn^{III}/Mn^{IV}=O) process and shifted + 50 mV the $E_{pa}2$ and $E_{pc}1$ of this quasi-reversible redox process. The shift of the Mn^{II}/Mn^{III} $E_{1/2}$ value to a more positive value favors the SOD activity of the porphyrin and the significant shift of the Mn^{III}/Mn^{IV}=O $E_{pc}1$ value makes the expected high valence species of the porphyrin resulting from the

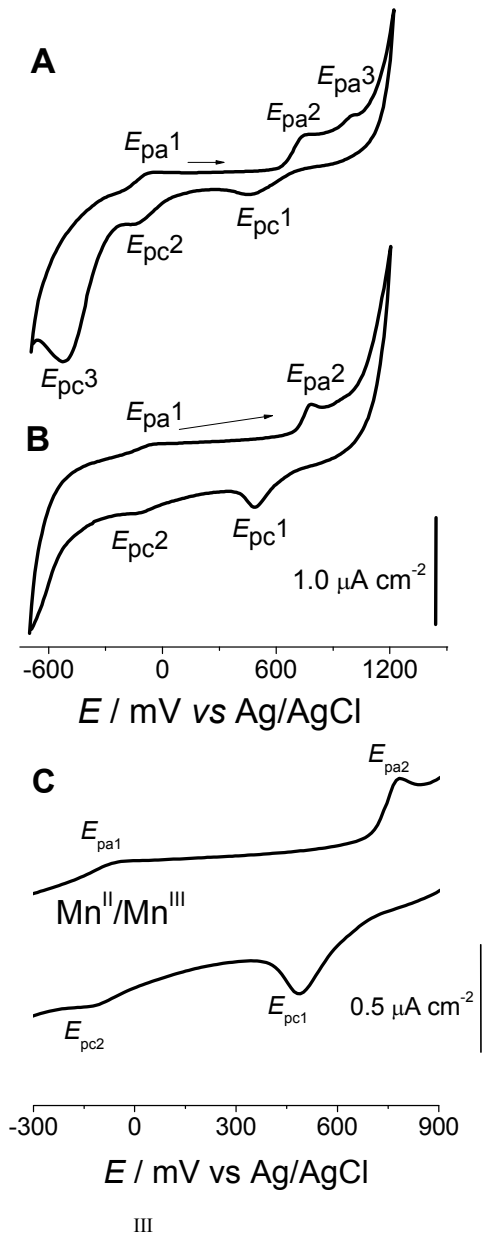

III

Fig. (6). Cyclic voltammograms of Mn^{III}TMPyP in the absence (**A**) and in the presence of PC/PS liposomes (**B**) obtained by using glass carbon in 5 mmol.L^{-1} phosphate buffer pH 7.4 at 100 mV/s rate. In **C** panel it is shown a zoom of the voltammogram obtained in the presence of PC/PS liposomes. The voltammograms were obtained by scanning the potential from the most negative to the most positive values and back, typically in the region of 0.6 to -0.6 V vs the $Ag/AgCl_{sat}$ electrode. The conversion of values obtained in mV vs $Ag/AgCl_{sat}$ to mV vs NHE was done by the addition of 197 to the values.

reaction with peroxides a more oxidative species prone to promote membrane oxidation. As an example, the redox potential of the Mn^{IV}=O/Mn^{III} in the PC/PS liposomes implicates that it is thermodynamically favorable for the oxidation of a PUFA-H (polyunsaturated fat acid bis-allylic-H) to PUFA$^{\bullet}$ (+600 mV *vs* NHE) [48-52]. In this regard, electrostatic binding of the hydrophilic porphyrin to the membrane surface is expected to favor a high PUFA-H/Mn^{III}TMPyP molar ratio in the membrane. On the other hand, even disregarding the positive shift of the Mn^{IV}=O/Mn^{III} potential promoted by PC/PS liposomes, in cells the recycling of the high valence state of the porphyrin to the resting form by GSH ($E_{1/2}$ = -220 mV *vs* NHE) [65,66] is thermodynamically favored. Peroxyl radicals have a wide range of reduction potentials (+770 to +1440 mV *vs* NHE) [65] and, in cells, some lipid-derived peroxides could contribute to the conversion of the high valence species of the porphyrin to the Mn^{III} resting form and also contribute to the propagation of lipid peroxidation. However, the reducing environment of the cytosol provided by NADPH and GSH makes improbable a significant contribution of peroxides to the recycling (conversion) of Mn^{III}TMPyP high valence species to the Mn^{III} resting form. Considering the redox potential values determined by the Mn^{III}/Mn^{II} and Mn^{IV}=O/Mn^{III} redox process, Mn^{III} resting form and Mn^{IV}=O, could contribute to the oxidation of $O_2^{\bullet-}$ to O_2. Considering the redox potential values, the $O_2^{\bullet-}/O_2$ couple (-330 mV *vs* NHE) and specially the protonated form, the perydroxyl radical ($E_{1/2}$ $HO_2^{\bullet}/O_2$ couple = -460 mV *vs* NHE), it is evident that these species are competitive with GSH and NADPH for the reduction of the porphyrin in cells [64,65]. However, it is important to consider that the cell system is heterogeneous with the reactants partitioned in different microenvironments and some reactions predicted as thermodynamically favorable by redox potential values can be disfavored by the product/reactant ratio. Particularly $HO_2^{\bullet}$ (pK_a = 4.8) is expected to be formed at the acid interface provided by acidic phospholipids such as PS and also by CL in the mitochondria and partitioned preferentially into the bilayer [67]. Therefore, $HO_2^{\bullet}$ is not expected to contribute significantly to the porphyrin reduction and so, NADPH and GSH are assigned as the principal reducing agents for the porphyrin.

The Reactivity of Mn^{III}TMPyP with Lipid-derived Peroxides

Mn^{III}TMPyP can react with residual lipid-derived peroxides formed by aging of the lipids during storage. The incubation of Mn^{III}TMPyP with PC/PS liposomes resulted in spectral changes consistent with the partial depletion of Mn^{III}TMPyP to generate the oxo manganesyl (Mn^{IV}=O) species and lipid-derived oxidized products (Fig. **7A**). The high valence state of Mn^{III}TMPyP results from the reaction of the porphyrin with residual peroxides. In this condition, the peculiar characteristics of (Mn^{IV}=O)TMPyP species observed in the presence of liposomes in comparison with those previously described for solution reaction of Mn^{III}TMPyP with peroxides [67] reinforces the fact that the porphyrin is bound to the membrane. The highly prominent ~ 270 nm peak appearing in the course of the reaction most probably results from the formation of lipid oxidized products such as conjugated ketone dienes [68-71]. The reaction rate was dependent on the lipid content (2.0 ± 0.3 ms^{-1} and 6 ± 1.2 ms^{-1} in the presence of 0.5 and 1.0 mmol.L^{-1} total lipid, respectively) and was not influenced by the addition of *t*-BuOOH (5.3 ± 1.1 ms^{-1} in the presence of 1.0 mmol.L^{-1} total lipid) (Fig. **7B**), probably due to the location

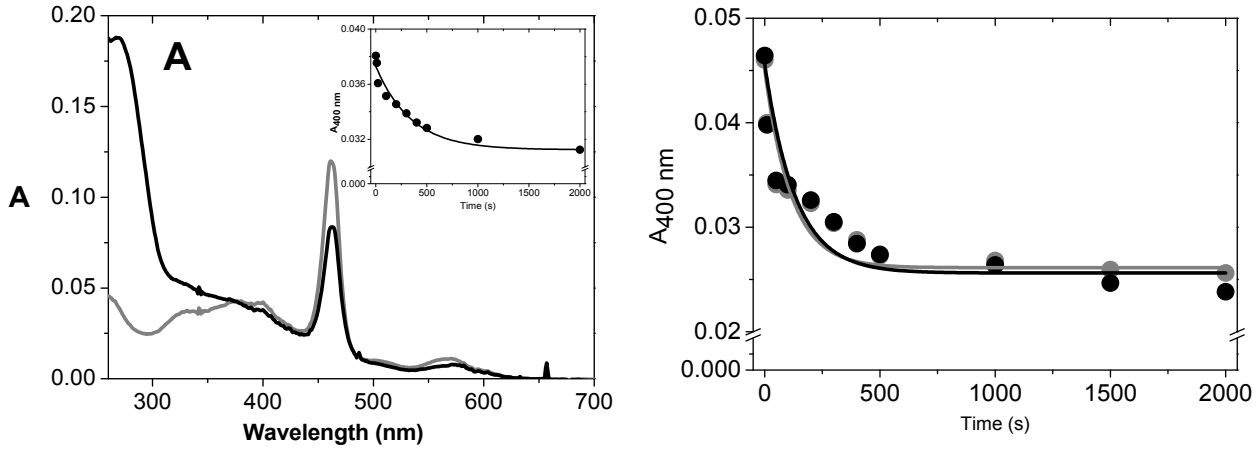

Fig. (7). Reaction of Mn^{III}TMPyP with peroxides. **A-** Spectral of Mn^{III}TMPyP before (gray line) and after (black line) incubation with PC/PS liposomes. The inset shows 400 nm absorbance decay during the incubation with PC/PS liposomes. **B-** Decay of absorbance at 400 nm during incubation with PC/PS liposomes (1.0 mmol.L^{-1} total lipid) in the absence (gray line and balls) and in the presence of *t*-BuOOH (black line and balls). The highly prominent ~ 270 nm peak that appeared in the course of the reaction (panel A) was assigned to conjugated ketone dienes. The reactions were carried out at 28°C, in 5 mmol.L^{-1} phosphate buffer, pH = 7.0 and in the presence of 2 μmol.L^{-1} porphyrin.

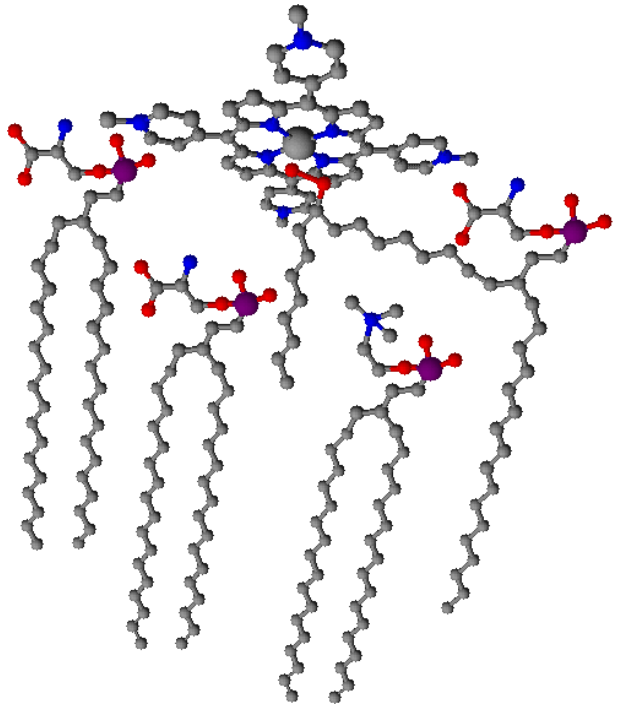

Fig. (8). Interaction of Mn^{III}TMPyP with PS molecules and with a peroxy-derived PS close to the metal center in bilayers containing also PC molecules (gray structure).

of the peroxide preferentially buried inside the bilayer. The spectral changes compatible with the formation of high valence species of Mn^{III}TMPyP were prevented by replacing PC/PS by DPPC/DPPS (not shown). These results are consistent with the reaction of the porphyrin with residual lipid-derived peroxides leading to generation of free radicals. The free radicals generated at the initial step trigger a chain reaction that generates additional peroxides that contributes to the conversion of a fraction of Mn^{III}TMPyP to the high valence state.

Fig. (**8**) illustrates the interaction of Mn^{III}TMPyP with PS molecules in bilayers containing also PC (gray structure). Fig. (**5**) shows also a peroxy-derived PS interacting with the porphyrin metal center.

CONCLUSIONS

Taken together the above results show that Mn^{III}TMPyP binds to the negatively charged membrane lipid, phosphatidylserine, *via* electrostatic interaction in a

cooperative way and the presence of saturated or unsaturated acyl chain in PS did not affect significantly the affinity to the membrane. The association to the acidic interface provided by PS changed the redox potentials of the Mn^{III}/Mn^{II} and Mn^{IV}/Mn^{III} couples to more positive values making the porphyrin metal center a better oxidizing agent. Thus Mn^{III}TMPyP promptly reacts with the surrounding lipid-derived peroxides and is converted to the high valence state. The Mn^{III}TMPyP used here is the *para* isomer which has previously been considered the less efficient form to act as SOD mimics. However, recently we have found this porphyrin was efficient to decrease the generation of superoxide ion in antimicyn A-poisoned mitoplasts [42]. The decrease of superoxide ion was accompanied by GSH depletion consistent with GPx-like activity. Therefore, the results presented here show the association of *para* Mn^{III}TMPyP with negatively charged membranes modulates the redox processes of the porphyrin toward a more efficient SOD activity than that expected from the values obtained in homogeneous media. However, different from SOD, membrane-bound Mn^{III}TMPyP can also react with lipid-derived peroxides and start lipid peroxidation propagation. The high valence species formed, the $(Mn^{IV}=O)$TMPyP, could be recycled to the Mn^{III} resting form by NADPH and GSH present in the cell. Additionally, Mn^{III}TMPyP can also be reduced by NADH and GSH and promote superoxide reduction to hydrogen peroxide by acting as NADH/GSH superoxide reductase, *i.e.*, with a semi-SOD activity. However, both of the reactions described above lead to depletion of the cell reducing agents and reinforce the previous conclusion that the antioxidant efficiency of Mn^{III}TMPyP is dependent on the NADPH/GSH content in cells.

CONFLICT OF INTEREST

The author(s) confirm that this article content has no conflicts of interest.

ACKNOWLEDGEMENTS

The authors are grateful to FAPESP (2008/04948-0, 2011/01541-0) CAPES and CNPq (475235/2010-0 and 304255/2010-6**)** for the financial support and to Professor Karl J. Jalkanen for the critical reading of the manuscript. We thank also to UFABC and CENAPAD-Campinas/SP (Centro Nacional de Processamento de Alto Desempenho) for the computational facilities.

REFERENCES

[1] Schroit, A.J.; Zwaal, R.F.A. Transbilayer movement of phospholipids in red cell and platelet membranes. *Biochim. Biophys. Acta*, **1991**, *1071*, 313-329.

[2] Devaux, P.F.; Zachowski, A. Maintenance and consequences of membrane phospholipid asymmetry. *Chem. Phys. Lipids*, **1994**, *73*, 107-120.

[3] Balasubramanian, K.; Schroit, A.J. Aminophospholipid asymmetry: a matter of life and death. *Annu. Rev. Physiol.*, **2003**, *65*, 701-734.

[4] Bevers, E.M.; Comfurius, P.; Dekkers, D.W.A.; Zwaal, R.F.A. Lipid translocation across the plasma membrane of mammalian cells. *Biochim. Biophys. Acta*, **1999**, 1439, 317-330.

[5] Pomorski, T.; Holthuis, J.C.M.; Herrmann, A.; van Meer, G. *J. Cell Sci.*, **2004**, *117*, 805-813.

[6] Pomorski, T.; Menon, A.K. Lipid flippases and their biological functions. *Cell. Mol. Life Sci.*, **2006**, *63*, 2908-2921.

[7] Zwaal, R.F.A.; Comfurius, P.; Bevers, E.M. Surface exposure of phosphatidylserine in pathological cells. *Cell Mol. Life Sci.*, **2005,** *62*, 971-988.

[8] Daleke, D.L. Phospholipid Flippases. *J. Biol. Chem.*, **2007**, 282, 821-825.

[9] Elliott, J.L.; Surprenant, A.; Marelli-Berg, F.M.; Cooper, J.C.; Cassady-Cain, R.L.; Wooding, C.; Linton, K.; Alexander, D.R.; Higgins, C.F. Membrane phosphatidylserine distribution as a non-apoptotic signalling mechanism in lymphocytes. *Nat. Cell Biol.*, **2005**, *7*, 808-816.

[10] Fadok, V.A.; Bratton, D.L.; Rose, D.M.; Pearson, A.; Ezekewitz, R.A.B.; Henson, P.M. A receptor for phosphatidylserine-specific clearance of apoptotic cells. *Nature*, **2000**, *405*, 85-90.

[11] Connor, J.; Pak, C.C.; Schroit, A.J. Exposure of phosphatidylserine in the outer leaflet of human red blood cells. Relationship to cell density, cell age, and clearance by mononuclear cells. *J. Biol. Chem.*, **1994**, *269*, 2399-2404.

[12] Cocco, R.E.; Ucker, D.S. Distinct Modes of Macrophage Recognition for Apoptotic and Necrotic Cells Are Not Specified Exclusively by Phosphatidylserine Exposure. *Mol. Biol. Cell*, **2001**, *12*, 919-930.

[13] Gadella, B.M.; Harrison, R.A. Capacitation induces cyclic adenosine 3',5'-monophosphate-dependent, but apoptosis-unrelated, exposure of aminophospholipids at the apical head plasma membrane of boar sperm cells. *Biol. Reprod.*, **2002,** *67*, 340-350.

[14] Duvall, E.; Wyllie, A.H.; Morris, R.G. Macrophage recognition of cells undergoing programmed cell death (apoptosis). *Immunology*, **1985**, *56*, 351-358.

[15] Gu, B.; Bendall, L.J.; Wiley, J.S. Adenosine triphosphate-induced shedding of CD23 and L-selectin (CD62L) from lymphocytes is mediated by the same receptor but different metalloproteases. *Blood*, **1998**, *92*, 946-951.

[16] Zwaal, R.F.; Schroit, A.J. Pathophysiologic implications of membrane phospholipid asymmetry in blood cells. *Blood*, **1997**, *15*, 1121-1132.

[17] Crowe, S.M.; Kornbluth, R.S. Overview of HIV interactions with macrophages and dendritic cells: the other infection in AIDS. *J. Leukoc. Biol.*, **1994**, *56*, 215-217.

[18] Rezende, S.M.; Simmonds, R.E.; Lane, D.A. Coagulation, inflammation, and apoptosis: different roles for protein S and the protein S–C4b binding protein complex. *Blood*, **2004**, *103*, 1192-1200.

[19] van den Eijnde, S.M.; van den Hoff, M.J.B.; Reutelingsperger, C.P.M.; van Heerde, W.L.; Henfling, M.E.R.; Vermeij-Keers, C.; Schutte, B.; Borgers, M.; Ramaekers, F.C.S. Transient expression of phosphatidylserine at cell-cell contact areas is required for myotube formation. *J. Cell. Sci.*, **2001**, *114*, 3631-3642.

[20] Marguet, D.; Luciani, M.F.; Moynault, A.; Williamson, P.; Chimini, G. Engulfment of apoptotic cells involves the redistribution of membrane phosphatidylserine on phagocyte and prey. *Nature Cell Biol.*, **1999**, *1*, 454-456.

[21] Frasch, S.C.; Henson, P.M.; Nagaosa, K.; Fessler, M.B.; Borregaard, N.; Bratton, D.L. Phospholipid flip-flop and phospholipid scramblase (PLSCR 1) co-localize to uropod rafts in formylated Met-Leu-Phe-stimulated neutrophils. *J. Biol. Chem.*, **2004**, *279*, 17625-17633.

[22] Sim, J.A.; Young, M.T.; Sung, H.-Y.; North, R.A.; Surprenant, A. Reanalysis of $P2X_7$ receptor expression in rodent brain. *J. Neurosci.*, **2004**, *24*, 6307-6314.

[23] Aramaki, Y.; Nitta, F.; Matsuno, R.; Morimura, Y.; Tsuchiya, S. Inhibitory effects of negatively charged liposomes on nitric oxide production from macrophages stimulated by LPS. *Biochem. Biophys. Res. Comm.*, **1996**, *220*, 1-6.

[24] Aramaki, Y.; Matsuno, R.; Tsuchiya, S. Involvement of p38 MAP kinase in the inhibitory effects of phosphatidylserine liposomes on nitric oxide production from macrophages stimulated with LPS. *Biochem. and Biophys. Res. Comm.*, **2001**, *280*, 982-987.

[25] Amirmansour, C.; Vallance, P.; Bogle, R.G. Tyrosine nitration in blood vessels occurs with increasing nitric oxide concentration. *Br. J. Pharmacol.*, **1999**, *127*, 788-794.

[26] Smith, R.A.; Balis, F.M.; Ott, K.H.; Elsberry, D.D.; Sherman, M.R.; Saifer, M.G. Pharmacokinetics and tolerability of ventricularly administered superoxide dismutase in monkeys and preliminary clinical observations in familial ALS. *J. Neurol. Sci.*, **1995**, *129*, 13-18.

[27] Jardot, G.; Vaille, A.; Maldonado, J.; Vanelle, P. Clinical pharmacokinetics and delivery of bovine superoxide dismutase. *Clin. Pharmacokinet.*, **1995**, 28, 17–25.

[28] Petkau, A. Scientific basis for the clinical use of superoxide dismutase. *Cancer Treat. Rev.*, **1986**, *13*, 17-44.

[29] Corominas, M.; Bas, J.; Romeu, A.; Valls, A.; Massip, E.; Gonzalez, L.; Mestre, M.; Buendia, E. Hypersensitivity reaction after orgotein (superoxide dismutase) administration. *Allergol. Immunopathol. (Madr.)*, **1990**, *18*, 297-299.

[30] McCord, J.M. Superoxide dismutase: Rationale for use in reperfusion injury and inflammation. *J. Free Radic. Biol. Med.*, **1988**, 2, 307–310.

[31] Huber, W. Orgotein - (bovine Cu-Zn superoxide dismutase), an anti-inflammatory protein drug: Discovery, toxicology and pharmacology. *Eur. J. Rheumatol. Inflamm.*, **1981**, *4*, 173-182.

[32] Salvemini, D.; Riley, D.P.; Cuzzocrea, S. SOD mimetics are coming of age. *Nat. Rev. Drug Discov.*, **2002**, *1*, 367-74.

[33] Pessoto, F.S.; Inada, N.M.; Nepomuceno, M.deF.; Ruggiero, A.C.; Nascimento, O.R.; Vercesi, A.E.; Nantes, I.L. Biological effects of anionic meso-tetrakis (*para*-sulfonatophenyl) porphyrins modulated by the metal center. Studies in rat liver mitochondria. *Chem. Biol. Interact.*, **2009,** *181*, 400-408.

[34] Batinic-Haberle I.; Rajic Z.; Tovmasyan A.; Reboucas J.S.; Ye X.; Leong K.W.; Dewhirst M.W.; Vujaskovic Z.; Benov L.; Spasojevic I. Diverse functions of cationic Mn(III) N-substituted pyridylporphyrins, recognized as SOD mimics. *Free Radic. Biol. Med.*, **2011**, *51*, 1035-1053.

[35] Spasojevic, I.; Batinic-Haberle, I.; Reboucas, J.S.; Idemori, Y.M.; Fridovich, I.J. Electrostatic contribution in the catalysis of O_2*-dismutation by superoxide dismutase mimics. Mn^{III}TE-2-PyP5+ versus Mn^{III}Br8T-2-PyP+. *Biol. Chem.*, **2003**, *278*, 6831-6837.

[36] Day, B.J.; Fridovich, I.; Crapo, J.D. Manganic porphyrins possess catalase activity and protect endothelial cells against hydrogen peroxide-mediated injury. *Arch. Biochem. Biophys.*, **1997**, *347*, 256-262.

[37] Simonson, S.G.; Welty-Wolf, K.E.; Huang, Y.C.; Taylor, D.E.; Kantrow, S.P.; Carraway, M.S.; Crapo, J.D.; Piantadosi, C.A. I. Physiology and biochemistry. *J. Appl. Physiol.*, **1997**, *83*, 550-558.

[38] Shaffer, S.G.; O'Neill, D.H.; Thibeault, D.W. Administration of bovine superoxide dismutase fails to prevent chronic pulmonary sequelae of neonatal oxygen exposure in the rat. *J. Pediatr.*, **1987**, *110*, 942-946.

[39] Stoyanovsky, D.A.; Huang, Z.; Jiang, J.; Belikova, N.A.; Tyurin, V.; Epperly, M.W.; Greenberger, J.S.; Bayir, H.; Kagan, V.E. A manganese–porphyrin complex decomposes H_2O_2, inhibits apoptosis, and acts as a radiation mitigator *in vivo*. *Med. Chem. Lett*, **2011**, *2*, 814-817.

[40] Araujo, J.C.; Pessoto, F.S.; Nascimento, O.R.; Nantes, I.L. Catalytic properties of *meso-tetrakis* porphyrins modulated by the metal center and meso ligands. Implications for biological effects. *Curr. Top. Biochem. Res.*, **2010**, *12*, 20–29.

[41] Nantes, I.L.; Durán, N.; Pinto, S.M.S.; Silva, F.B.; Souza, J.S.; Isoda, N.; Luz, R.A.S.; Oliveira, T.G.; Fernandes, V.G. Modulation of the catalytic activity of porphyrins by lipid- and surfactant-containing nanostructures. *J. Braz. Chem. Soc.*, **2011**, *22*, 1621-1633.

[42] Araujo-Chaves, J.C.; Yokomizo, C.H.; Kawai, C.; Mugnol, K.C.U.; Prieto, T.; Nascimento, O.R.; Nantes, I.L. Towards the mechanisms involved in the antioxidant action of Mn^{III} [meso-tetrakis(4-N-methyI pyridinium) porphyrin] in mitochondria. *J. Bioenerg. Biomembr.*, **2011**, *43*, 663-671.

[43] Ferrer-Sueta, G.; Vitturi, D.; Batinic-Haberle, I.; Fridovich, I.; Goldstein, S.; Czapski, G.; Radi, R. Reactions of manganese porphyrins with peroxynitrite and carbonate radical anion. *J. Biol. Chem.*, **2003**, *278*, 27432-27438.

[44] Batinic´-Haberle, I.; Benov, L.; Spasojevic, I.; Fridovich, I. The ortho effect makes manganese(III) meso-tetrakis(N-methylpyridinium-2-yl)porphyrin a powerful and potentially useful superoxide dismutase mimic. *J. Biol. Chem.*, **1998**, *273*, 24521-24528.

[45] Batinić-Haberle, I.; Rebouças, J.S.; Spasojević, I. Superoxide dismutase mimics: chemistry, pharmacology, and therapeutic potential. *Antioxid. Redox Signal.*, **2010**, *15*, 877-918.

[46] Nagami, H.; Umakoshi, H.; Shimanouchi, T.; Kuboi, R. Variable SOD-like activity of liposome modified with Mn(II)–porphyrin derivative complex. *Biochem. Eng. J.*, **2004**, *21*, 221-227.

[47] Kagan, V.E.; Fabisiak, J.P.; Shvedova, A.A.; Tyurina, Y.Y.; Tyurin, V.A.; Schor, N.F.; Kawai, K. Oxidative signaling pathway for externalization of plasma membrane phosphatidylserine during apoptosis. *FEBS Lett.*, **2000**, *477*, 1-7.

[48] Fariss, M.W.; Chan, C.B.; Patel, M.; Van Houten, B.; Orrenius, S. Role of mitochondria in toxic oxidative stress. *Mol. Interv.*, **2005**, *5*, 94-111.

[49] Kresse, G.; Joubert, D. From ultrasoft pseudopotentials to the projector augmented-wave method. *Phys. Rev. B.*, **1999**, *59*, 1758-1775.

[50] Blochl, P.E. Projector augmented-wave method. *Phys. Rev. B.*, **1994**, *50*, 17953–17979.

[51] Mugnol, K.C.U.; Martins, M.V.A.; Nascimento, E.C.; Nascimento, O.R.; Crespilho, F.N.; Arantes, J.T.; Nantes, I.L. Interaction of Fe3+meso-tetrakis (2,6-dichloro-3-sulfonatophenyl) porphyrin with cationic bilayers: magnetic switching of the porphyrin and magnetic induction at the interface. *Theor. Chem. Acc.*, **2011,** *130*, 829-837.

[52] Nantes, I.L.; Mugnol, K.C.U. Incorporation of Respiratory Cytochromes in Liposomes: An Efficient Strategy to Study the Respiratory Chain. *J. Lipos. Res.*, **2008**, 18, 175-94.

[53] Nantes, I.L.; Crespilho, F.N.; Mugnol, K.C.U.; Araújo-Chaves, J.C.; Luz, R.A.S.; Nascimento, O.R.; Pinto, S.M.S. Magnetic circular dichroism applied in the study of symmetry and functional properties of porphyrinoids. In: *Circular Dichroism: Theory and Spectroscopy*; Rodgers, D.S., Ed. *Nova Science Publishers*, Inc.: Hauppauge, New York, **2010**.

[54] Nantes, I.L.; Crespilho, F.N.; Nascimento, O.R.; Mugnol, K.C.U.; Araújo-Chaves, J.C.; Luz, R.A.S.; Pinto, S.M.S. Effect of the medium, supramolecular organization and association with colloidal systems on the UV-visible and magnetic circular dichroism spectra of porphyrinoids. *Chem. Phys. Res. J.*, **2011**, 4, issue 3, (ISSN: 1935-2492), in Press.

[55] Hao, Y.; Sek-Wen, H. Merocyanine 540 as a probe to monitor the molecular packing of phosphatidylcholine, a monolayer epifluorescence microscopy and spectroscopy study. *Biochim. Biophys. Acta*, **1992,** *1107*, 245-254.

[56] Jalkanen, K.J.; Degtyarenko, I.M.; Nieminen, R.M.; Cao, X.; Nafie, L.A.; Zhu F.; Barron, L.D. Role of hydration in determining the structure and vibrational spectra of L-alanine and N-acetyl L-alanine N'-methylamide in aqueous solution: A combined theoretical and experimental study. *Theor. Chem. Acc.*, **2008**, *119*, 191-210.

[57] Carmona-Ribeiro, A.M. Interactions between charged spheric vesicles. *J. Phys. Chem.*, **1993**, *97*, 1183-11846.

[58] Verkman, A.S.; Frosch. M.P. Temperature-jump studies of merocyanine 540 relaxation kinetics in lipid bilayer membranes. *Biochemistry*, **1985**, *24*, 7117-7122.

[59] Tsui, F.C.; Ojcius, D.M.; Hubbell, W.L. The intrinsic pKa values for phosphatidylserine and phosphatidylethanolamine in phosphatidylcholine host bilayers. *Biophysical J.*, **1986**, *49*, 459-468.

[60] Batinic´-Haberle, I.; Spasojevic´, I.; Hambright, P.; Benov, L.; Crumbliss, A.L.; Fridovich, I. Relationship among redox potentials, proton dissociation constants of pyrrolic nitrogens, and *in vivo* and *in vitro* superoxide mismutating activities of manganese(III) and iron(III) water-soluble porphyrins. *Inorg. Chem.*, **1999**, *38*, 4011-4022.

[61] Jovanovic, S.V.; Jankovic, I.; Josimovic, L. Electron-transfer reactions of alkyl peroxy radicals. *J. Am. Chem. Soc.*, **1992**, *114*, 9018-9021.

[62] Tan, D.-x.; Livrea, M.A.; Reiter, R.J.; Tesoriere, L. Radical and reactive intermediate-scavenger properties of melatonin in pure chemical systems. In: *Handbook of Antioxidants*; Cadenas, E.; Packer, L., Eds.; Marcel Dekker: New York, **2001**, pp. 615-632.

[63] Oliw, E.H.; Jerneréna, F.; Hoffmann, I.; Sahlin, M.; Garscha, U. Manganese lipoxygenase oxidizes bis-allylic hydroperoxides and octadecenoic acids by different mechanism. *Biochim. Biophys. Acta*, **2011**, *1811*, 138-147.

[64] Reipa, V. Direct spectroelectrochemical titration of glutathione. *Bioelectrochem.*, **2004**, 65, 47-49.

[65] Buettner, G.R. The pecking order of free radicals and antioxidants: lipid peroxidation, alpha-tocopherol, and ascorbate. *Arch. Biochem. Biophys.*, **1993**, *300*, 535-543.

[66] Chin, D-H.; Chiericato Jr., G.; Nanni Jr., E.J.; Sawyer, D.T. Proton-induced disproportionation of superoxide ion in aprotic media. *J. Am. Chem. Soc.*, **1982**, *104*, 1296-1299.

[67] Marla, S.S.; Lee, J.; Groves, J.T. Peroxynitrite rapidly permeates phospholipid membranes *Proc. Natl. Acad. Sci. USA*, **1997**, *94*, 14243-14248.

[68] Goel, S.K.; Lalwani, N.D.; Reddy, J.K. Peroxisome proliferation and lipid peroxidation in rat liver. *Cancer Res.*, **1986**, *46*, 1324-1330.

[69] Recknagel, R.O.; Glende, E.A., Waller Jr., R.L.; Lowrey, K. Lipid peroxidation: biochemistry measurement and significance in liver cell injury. In: *Toxicology of the Liver*; Plaa, G.L.; Hewitt, W.R., Eds.; Raven Press: New York, **1982**, pp. 213-241.

[70] Holman, R.T. Autoxidation of fats and related substances. *Prog. Chem. Fats other Lipids*, **954**, *2*, 51-98.

[71] Hess, H.H.; Thalheimer, C. Microassay of biochemical structural components in nervous tissues. I. Extraction and partition of lipids and assay of nucleic acids. *J. Neurochem.*, **1965**, *72*, 193-204.

Received: January 07, 2012 **Revised: May 03, 2012** **Accepted: May 17, 2012**